Proceedings of the 8th IEEE Mediterranean Conference
on Control and Automation (MED 2000)
Rio, Patras, GREECE 17-19 July, 2000

A H_∞ design procedure for position tracking control of current-fed induction motors

Stefano Chiaverini and Giuseppe Fusco

Dipartimento di Automazione, Elettromagnetismo, Ingegneria dell'Informazione e Matematica Industriale
Università degli Studi di Cassino, via G. Di Biasio 43, 03043 Cassino (FR), Italy

Key Words: Electro-mechanical systems; H_∞ control; Tracking control; Feedback linearization.

Abstract

This paper gives a systematic procedure to designing H_∞ position tracking controller for current-fed induction motors. The proposed method assumes that stator currents and rotor position measurements are available while rotor flux components are determined by means of a reduced-order observer. The H_∞ controller yields convergence to zero of both position and flux norm tracking errors while ensuring robustness with respect to load torque disturbances. The interesting feature of this method is that it enables to determine the capability rejection of the controller in function of the bandwidth's value imposed on the control system. Hence, it represents a powerful design tool because it gives a criterium for the choice of the best rejection value achievable by the H_∞ controller. To test the robustness of the proposed control scheme, a position tracking control problem for an induction motor actuating a single-link robotic load is considered. Simulation results are also included which confirm the effectiveness of the proposed procedure.

1 Introduction

A typical application for an induction motor is its use as actuator for electromechanical systems aimed at tracking a time varying desired trajectory. However the tracking position control is made difficult due to the induction motor being a multivariable system with coupled and nonlinear dynamics. In addition, full state measurements are usually not available. Hence, several researchers have investigated the use of feedback linearization and/or adaptive control techniques for the position control of induction motors without rotor velocity or rotor flux measurements, even in presence of parametric uncertainty associated with rotor resistance value (see, e.g., [1, 5, 7, 12]). Nevertheless, the design of these controllers requires a complex mathematical development. In particular, some papers have investigated the design of a tracking position controller for an induction motor whose mechanical load is represented by a robot manipulator (see, e.g., [2, 10]).

Recently, a different approach to the position control problem of induction motors has led to the development of robust controllers which minimize a generalized energy cost function, including the power losses and/or the stored magnetic energy, while satisfying robust control objectives [3, 4, 8, 9]. In this context, a good controller is one that achieves effective disturbance rejection with low energy consumption. This point of view leads to the definition of a control problem in the framework of the H_∞ control theory.

In this paper, a position tracking H_∞ controller is designed through the adoption of a systematic procedure. This controller yields convergence to zero of both position and flux norm tracking errors while ensuring robustness with respect to load torque disturbances. The proposed procedure design requires stator currents, rotor position measurements and exact model knowledge, while the flux components are estimated from a reduced-order observer. The interesting feature of this approach is that the capabilities rejection of the H_∞ controller are numerically obtained as a function of the bandwidth's values of the control system. Hence, starting from the desired bandwidth's value, the best capability rejection achievable from the controller is easily determined together with the controller gains. It is worth noting that the admissible value of the control system bandwidth must be chosen according to the sampling frequency of the digital control architecture required for the implementation of the control law. Simulation results are presented to illustrate the effectiveness of the proposed approach applied to the position control of an induction motor driving a one-link robot manipulator.

2 Induction motor model and problem formulation

The model of a current-fed induction motor in a α-β reference frame, fixed to the stator, can be represented as:

$$\begin{cases} \dfrac{\mathrm{d}\phi_{r\alpha}}{\mathrm{d}t} = -\dfrac{R_r}{L_r}\,\phi_{r\alpha} - \omega\,\phi_{r\beta} + M\dfrac{R_r}{L_r}\,i_{s\alpha} \\ \dfrac{\mathrm{d}\phi_{r\beta}}{\mathrm{d}t} = \omega\,\phi_{r\alpha} - \dfrac{R_r}{L_r}\,\phi_{r\beta} + M\dfrac{R_r}{L_r}\,i_{s\beta} \\ \dfrac{\mathrm{d}\omega}{\mathrm{d}t} = \dfrac{k_T}{J}(\phi_{r\alpha}\,i_{s\beta} - \phi_{r\beta}\,i_{s\alpha}) - \dfrac{T_l}{J} \end{cases} \tag{1}$$

where R_r and L_r respectively denote the rotor resistance and self-inductance, M is the mutual inductance, J is the total inertia seen at the rotor axis, T_l is the unknown load torque, $k_T = pM/L_r$ is the electromagnetic torque constant, and p is the number of pole pairs; the subscripts s and r stand for stator and rotor. In (1)

the control inputs are the α-β components of the stator currents $(i_{s\alpha}, i_{s\beta})$; the state variables are the α-β components of the rotor flux $(\phi_{r\alpha}, \phi_{r\beta})$ and the rotor speed (ω).

Defining the norm of the rotor flux as

$$\phi = \sqrt{\phi_{r\alpha}^2 + \phi_{r\beta}^2},$$

and choosing the stator currents according to the following state-feedback control law [12]

$$\begin{pmatrix} i_{s\alpha} \\ i_{s\beta} \end{pmatrix} = \frac{1}{\phi^2} \begin{pmatrix} \phi\,\phi_{r\alpha} & -\phi_{r\beta} \\ \phi\,\phi_{r\beta} & \phi_{r\alpha} \end{pmatrix} \begin{pmatrix} u_\phi \\ u_T \end{pmatrix}, \qquad (2)$$

the nonlinear and coupled dynamics (1) can be described in terms of the linear and decoupled dynamics

$$\begin{cases} \dfrac{\mathrm{d}\phi}{\mathrm{d}t} = -\dfrac{R_r}{L_r}\phi + \dfrac{R_r}{L_r} M u_\phi \\ \dfrac{\mathrm{d}\omega}{\mathrm{d}t} = \dfrac{k_T}{J} u_T - \dfrac{T_l}{J} \end{cases} \qquad (3)$$

where u_ϕ and u_T are two new control inputs.

Notice that the implementation of (2) requires the knowledge of the rotor flux components which are not directly measurable; to this aim an observer will be introduced in the control scheme.

Since the objective of this paper is to design a rotor position tracking controller for the model given by (3), we define the flux norm, rotor position and velocity tracking errors as follows:

$$\epsilon_\phi = \phi_{\mathrm{ref}} - \phi \qquad \epsilon_\theta = \theta_{\mathrm{ref}} - \theta \qquad \epsilon_\omega = \omega_{\mathrm{ref}} - \omega \quad (4)$$

where ϕ_{ref}, θ_{ref} and ω_{ref} represent the desired rotor flux norm, position and velocity trajectories, respectively, and θ is the angular position of the rotor. The control objective is to make equal to zero, at the steady state, the errors (4); for this reason, two integral actions on the flux norm and rotor position tracking errors will be provided by means of two additional state variables ξ and η such that:

$$\frac{\mathrm{d}\xi}{\mathrm{d}t} = \epsilon_\phi \qquad \frac{\mathrm{d}\eta}{\mathrm{d}t} = \epsilon_\theta. \qquad (5)$$

The system (3), together with (4) and (5), can be rewritten in the following form:

$$\begin{cases} \dfrac{\mathrm{d}\epsilon_\phi}{\mathrm{d}t} = -\dfrac{R_r}{L_r}\epsilon_\phi + \dfrac{\mathrm{d}\phi_{\mathrm{ref}}}{\mathrm{d}t} + \dfrac{R_r}{L_r}\phi_{\mathrm{ref}} - \dfrac{R_r}{L_r} M u_\phi \\ \dfrac{\mathrm{d}\xi}{\mathrm{d}t} = \epsilon_\phi \\ \dfrac{\mathrm{d}\epsilon_\omega}{\mathrm{d}t} = \dfrac{\mathrm{d}\omega_{\mathrm{ref}}}{\mathrm{d}t} + \dfrac{T_l}{J} - \dfrac{k_T}{J} u_T \\ \dfrac{\mathrm{d}\epsilon_\theta}{\mathrm{d}t} = \epsilon_\omega \\ \dfrac{\mathrm{d}\eta}{\mathrm{d}t} = \epsilon_\theta \end{cases} \qquad (6)$$

This system can be divided in two decoupled subsystems; the first one obtained from the first two equations in (6), that will be called *electrical subsystem* and denoted by Σ_{el}, and the second one obtained from the last three equations in (6), that will be called *mechanical subsystem* and denoted by Σ_{mec}. It is simple to recognize that the electrical and the mechanical subsystems have the same form. In fact, the former can expressed as:

$$\Sigma_{\mathrm{el}} : \quad \dot{\boldsymbol{\rho}}_{\mathrm{el}} = \boldsymbol{A}_{\mathrm{el}}\boldsymbol{\rho}_{\mathrm{el}} + \boldsymbol{B}_{1,\mathrm{el}} w_{\mathrm{el}} + \boldsymbol{B}_{2,\mathrm{el}} u_\phi, \qquad (7)$$

where

$$\boldsymbol{\rho}_{\mathrm{el}} = \begin{pmatrix} \epsilon_\phi \\ \xi \end{pmatrix} \qquad w_{\mathrm{el}} = \dot{\phi}_{\mathrm{ref}} + \frac{R_r}{L_r}\phi_{\mathrm{ref}}$$

$$\boldsymbol{A}_{\mathrm{el}} = \begin{pmatrix} -R_r/L_r & 0 \\ 1 & 0 \end{pmatrix}$$

$$\boldsymbol{B}_{1,\mathrm{el}} = \begin{pmatrix} 1 \\ 0 \end{pmatrix} \qquad \boldsymbol{B}_{2,\mathrm{el}} = \begin{pmatrix} -M R_r/L_r \\ 0 \end{pmatrix},$$

while the latter becomes:

$$\Sigma_{\mathrm{mec}} : \quad \dot{\boldsymbol{\rho}}_{\mathrm{mec}} = \boldsymbol{A}_{\mathrm{mec}}\boldsymbol{\rho}_{\mathrm{mec}} + \boldsymbol{B}_{1,\mathrm{mec}}\boldsymbol{w}_{\mathrm{mec}} + \boldsymbol{B}_{2,\mathrm{mec}} u_T, \qquad (8)$$

where

$$\boldsymbol{\rho}_{\mathrm{mec}} = \begin{pmatrix} \epsilon_\omega \\ \epsilon_\theta \\ \eta \end{pmatrix} \qquad \boldsymbol{w}_{\mathrm{mec}} = \begin{pmatrix} \dot{\omega}_{\mathrm{ref}} \\ T_l \end{pmatrix}$$

$$\boldsymbol{A}_{\mathrm{mec}} = \begin{pmatrix} 0 & 0 & 0 \\ 1 & 0 & 0 \\ 0 & 1 & 0 \end{pmatrix}$$

$$\boldsymbol{B}_{1,\mathrm{mec}} = \begin{pmatrix} 1 & 1/J \\ 0 & 0 \\ 0 & 0 \end{pmatrix} \qquad \boldsymbol{B}_{2,\mathrm{mec}} = \begin{pmatrix} -k_T/J \\ 0 \\ 0 \end{pmatrix}.$$

Since the electrical and the mechanical subsystems dynamics can be expressed in the same form

$$\dot{\boldsymbol{\rho}} = \boldsymbol{A}\boldsymbol{\rho} + \boldsymbol{B}_1\boldsymbol{w} + \boldsymbol{B}_2\boldsymbol{u}, \qquad (9)$$

the H_∞ design of the position tracking controller can be performed, for each of the two subsystems, according to the following steps [6]:

- Define the subsystem output

$$\boldsymbol{z} = \boldsymbol{C}\boldsymbol{\rho} + \boldsymbol{D}\boldsymbol{u}, \qquad (10)$$

  in which the matrix $\boldsymbol{D}$ is such that the matrix $(\boldsymbol{D}^{\mathrm{T}}\boldsymbol{D})^{-1}$ is not singular.

- Solve, with respect to the unknown symmetric and positive definite matrix $\boldsymbol{X}$, the matrix Riccati's equation

$$\boldsymbol{H}(\boldsymbol{X},\gamma) = \boldsymbol{X}\widetilde{\boldsymbol{A}} + \widetilde{\boldsymbol{A}}^{\mathrm{T}}\boldsymbol{X} + \boldsymbol{X}\widetilde{\boldsymbol{B}}(\gamma)\boldsymbol{X} + \widetilde{\boldsymbol{C}}^{\mathrm{T}}\widetilde{\boldsymbol{C}} = \boldsymbol{O}, \qquad (11)$$

  in which

$$\begin{aligned} \widetilde{\boldsymbol{A}} &= \boldsymbol{A} - \boldsymbol{B}_2(\boldsymbol{D}^{\mathrm{T}}\boldsymbol{D})^{-1}\boldsymbol{D}^{\mathrm{T}}\boldsymbol{C} \\ \widetilde{\boldsymbol{B}}(\gamma) &= \frac{1}{\gamma^2}\boldsymbol{B}_1\boldsymbol{B}_1^{\mathrm{T}} - \boldsymbol{B}_2(\boldsymbol{D}^{\mathrm{T}}\boldsymbol{D})^{-1}\boldsymbol{B}_2^{\mathrm{T}} \\ \widetilde{\boldsymbol{C}} &= (\boldsymbol{I} - \boldsymbol{D}(\boldsymbol{D}^{\mathrm{T}}\boldsymbol{D})^{-1}\boldsymbol{D}^{\mathrm{T}})\boldsymbol{C} \end{aligned}$$

  where $\boldsymbol{O}$ and $\boldsymbol{I}$ respectively are the null matrix and the identity matrix of proper dimension, and γ^2 is the attenuation factor giving a measure of the capability of the controller to reject the effects of the disturbances on the system's output.

- Compute the control input as

$$\boldsymbol{u} = \boldsymbol{K}\boldsymbol{\rho}, \tag{12}$$

where:

$$\boldsymbol{K} = -(\boldsymbol{D}^{\mathrm{T}}\boldsymbol{D})^{-1}(\boldsymbol{B}_2^{\mathrm{T}}\boldsymbol{X} + \boldsymbol{D}^{\mathrm{T}}\boldsymbol{C}). \tag{13}$$

For each of the two considered subsystems, the interval of the admissible values of γ, ensuring the existence of a solution to (11), must be determined. In this way, for a desired admissible value of γ, the Riccati's matrix equation is solved, whose solution $\boldsymbol{X}$ is used in (13) to compute the matrix gain $\boldsymbol{K}$. Finally, the control inputs u_ϕ and u_T, which attenuate the effects of the external disturbances w_{el} and $\boldsymbol{w}_{\mathrm{mec}}$ and guarantee internal stability, are obtained from (12).

3 H_∞ design methodology for the electrical and mechanical subsystems

Let consider the subsystem Σ_{el} described by model (7) and the following output function

$$\boldsymbol{z}_{\mathrm{el}} = \begin{pmatrix} 1 & 0 \\ 0 & 1 \end{pmatrix} \begin{pmatrix} \epsilon_\phi \\ \xi \end{pmatrix} + \begin{pmatrix} d_{\mathrm{el}} \\ d_{\mathrm{el}} \end{pmatrix} u_\phi \tag{14}$$

with $d_{\mathrm{el}} \in \Re$. The matrices which appear in the equation (11) in this case become

$$\begin{aligned} \widetilde{\boldsymbol{A}} &= \begin{pmatrix} \frac{R_r}{L_r}(-1 + \frac{M}{2d_{\mathrm{el}}}) & \frac{R_r}{L_r}\frac{M}{2d_{\mathrm{el}}} \\ 1 & 0 \end{pmatrix} \\ \widetilde{\boldsymbol{B}}(\gamma_{\mathrm{el}}) &= \begin{pmatrix} 2\rho_{\mathrm{el}}^2\lambda & 0 \\ 0 & 0 \end{pmatrix} \\ \widetilde{\boldsymbol{C}} &= \begin{pmatrix} 1/2 & -1/2 \\ -1/2 & 1/2 \end{pmatrix} \end{aligned} \tag{15}$$

where

$$\rho_{\mathrm{el}} = \frac{R_r}{L_r}\frac{M}{2d_{\mathrm{el}}} \tag{16}$$

$$\lambda = \frac{1}{2\rho_{\mathrm{el}}^2\gamma_{\mathrm{el}}^2} - 1. \tag{17}$$

Notice that the function $\lambda(\gamma_{\mathrm{el}})$ is monotonically decreasing for $\gamma_{\mathrm{el}} > 0$; therefore, minimizing γ_{el} corresponds to maximizing λ.

Denoting the elements of the matrices $\boldsymbol{X}$ and $\boldsymbol{H}$ as

$$\boldsymbol{X} = \begin{pmatrix} x_1 & x_2 \\ x_2 & x_3 \end{pmatrix} \qquad \boldsymbol{H} = \begin{pmatrix} h_1 & h_2 \\ h_2 & h_3 \end{pmatrix}$$

and substituting the expressions (15) in (11) gives

$$\begin{cases} h_1 = \dfrac{1}{2} - 2\left(\dfrac{R_r}{L_r} - \rho_{\mathrm{el}}\right)x_1 + 2x_2 + 2\rho_{\mathrm{el}}^2\lambda x_1^2 = 0 \\ h_2 = -\dfrac{1}{2} + \rho_{\mathrm{el}}x_1 - \left(\dfrac{R_r}{L_r} - \rho_{\mathrm{el}}\right)x_2 + x_3 \\ \qquad +2\rho_{\mathrm{el}}^2\lambda x_1 x_2 = 0 \\ h_3 = \dfrac{1}{2} + 2\rho_{\mathrm{el}}x_2 + 2\rho_{\mathrm{el}}^2\lambda x_2^2 = 0 \end{cases} \tag{18}$$

The control design problem requires to find the maximum value of λ such that a triple $\{x_1, x_2, x_3\}$ exists which solves (18) and leads to a positive definite matrix $\boldsymbol{X}$. It is worth noting that, in view of (17), the parameter λ satisfies the constraint

$$\lambda > -1,$$

while it is

$$\lambda \leq 1$$

since the elements of the matrix $\boldsymbol{X}$ must belong to $\Re$. For $\lambda \in \Lambda =]-1, 1]$, the solution of system (18) can be expressed in the form [4]:

$$\begin{aligned} x_2 &= \frac{-1 \pm \sqrt{1-\lambda}}{2\lambda\rho_{\mathrm{el}}} \\ x_1 &= \frac{(\frac{R_r}{Lr} - \rho_{\mathrm{el}}) \pm \sqrt{(\frac{R_r}{Lr} - \rho_{\mathrm{el}})^2 - \lambda\rho_{\mathrm{el}}^2(1+4x_2)}}{2\lambda\rho_{\mathrm{el}}^2} \\ x_3 &= \frac{1}{2} - \rho_{\mathrm{el}}x_1 - (\rho_{\mathrm{el}} - \frac{R_r}{Lr})x_2 - 2\lambda\rho_{\mathrm{el}}^2 x_1 x_2. \end{aligned} \tag{19}$$

which enables a simple numerical computation of the functions $x_1(\lambda)$ and $|\boldsymbol{X}(\lambda)|$ in Λ.

Let now consider the subsystem Σ_{mec} described by (8), where the following output function is assumed

$$\boldsymbol{z}_{\mathrm{mec}} = \begin{pmatrix} 1 & 0 & 0 \\ 0 & 1 & 0 \\ 0 & 0 & 1 \end{pmatrix} \begin{pmatrix} \epsilon_\omega \\ \epsilon_\theta \\ \eta \end{pmatrix} + \begin{pmatrix} d_{\mathrm{mec}} \\ d_{\mathrm{mec}} \\ d_{\mathrm{mec}} \end{pmatrix} u_T \tag{20}$$

with $d_{\mathrm{mec}} \in \Re$. The matrices which appear (11) become

$$\begin{aligned} \widetilde{\boldsymbol{A}} &= \begin{pmatrix} k_T/3d_{\mathrm{mec}}J & k_T/3d_{\mathrm{mec}}J & k_T/3d_{\mathrm{mec}}J \\ 1 & 0 & 0 \\ 0 & 1 & 0 \end{pmatrix} \\ \widetilde{\boldsymbol{B}}(\gamma_{\mathrm{mec}}) &= \begin{pmatrix} \delta\rho_{\mathrm{mec}}^2 & 0 & 0 \\ 0 & 0 & 0 \\ 0 & 0 & 0 \end{pmatrix} \\ \widetilde{\boldsymbol{C}} &= \frac{1}{3}\begin{pmatrix} 2 & -1 & -1 \\ -1 & 2 & -1 \\ -1 & -1 & 2 \end{pmatrix} \end{aligned} \tag{21}$$

where

$$\rho_{\mathrm{mec}} = \frac{k_T}{\sqrt{6}\,J\,d_{\mathrm{mec}}} \tag{22}$$

$$\delta = \frac{1 + 1/J^2}{\rho_{\mathrm{mec}}^2\gamma_{\mathrm{mec}}^2} - 2. \tag{23}$$

Notice that the function $\delta(\gamma_{\mathrm{mec}})$ is monotonically decreasing for $\gamma_{\mathrm{mec}} > 0$; therefore, minimizing γ_{mec} corresponds to maximizing δ. In this case, the elements of the matrices $\boldsymbol{X}$ and $\boldsymbol{H}$ are denoted as:

$$\boldsymbol{X} = \begin{pmatrix} x_1 & x_2 & x_3 \\ x_2 & x_4 & x_5 \\ x_3 & x_5 & x_6 \end{pmatrix} \qquad \boldsymbol{H} = \begin{pmatrix} h_1 & h_2 & h_3 \\ h_2 & h_4 & h_5 \\ h_3 & h_5 & h_6 \end{pmatrix}$$

According to the above procedure, substituting the expressions (21) in (11) gives

$$\begin{cases} h_1 = \frac{2}{3} + \frac{2}{3}\frac{k_T}{d_{\rm mec}J}x_1 + \delta\rho^2_{\rm mec}x_1^2 + 2x_2 = 0 \\ h_2 = -\frac{1}{3} + \frac{1}{3}\frac{k_T}{d_{\rm mec}J}x_1 + \frac{1}{3}\frac{k_T}{d_{\rm mec}J}x_2 + \delta\rho^2_{\rm mec}x_1x_2 \\ \quad +x_3 + x_4 = 0 \\ h_3 = -\frac{1}{3} + \frac{1}{3}\frac{k_T}{d_{\rm mec}J}x_1 + \frac{1}{3}\frac{k_T}{d_{\rm mec}J}x_3 + \delta\rho^2_{\rm mec}x_1x_3 \\ \quad +x_5 = 0 \\ h_4 = \frac{2}{3} + \frac{2}{3}\frac{k_T}{d_{\rm mec}J}x_2 + \delta\rho^2_{\rm mec}x_2^2 + 2x_5 = 0 \\ h_5 = -\frac{1}{3} + \frac{1}{3}\frac{k_T}{d_{\rm mec}J}x_2 + \frac{1}{3}\frac{k_T}{d_{\rm mec}J}x_3 + \delta\rho^2_{\rm mec}x_2x_3 \\ \quad +x_6 = 0 \\ h_6 = \frac{2}{3} + \frac{2}{3}\frac{k_T}{d_{\rm mec}J}x_3 + \delta\rho^2_{\rm mec}x_3^2 = 0 \end{cases} \tag{24}$$

The objective of the control design problem is to find the maximum value of δ such that a sextuple $\{x_1, x_2, x_3, x_4, x_5, x_6\}$ exists which solves (24) and leads to a positive definite matrix $\boldsymbol{X}$. Notice that, in view of (23), the parameter δ satisfies the constraint

$$\delta > -2,$$

while it is

$$\delta \leq 1$$

since the elements of the matrix $\boldsymbol{X}$ must belong to $\Re$. For a given δ, a solution to the system (24) can be found as follows: The first equation in (24) is used to express x_2 as a function of x_1. Then, the last equation in (24) is solved with respect to the unknown x_3; let $x_{3,1}$ and $x_{3,2}$ be the two solutions. At this point, by substituting e.g. $x_{3,1}$ in the third equation in (24), we can express x_5 as a function of x_1. Plugging the obtained expressions of $x_2(x_1)$ and $x_5(x_1)$ into the fourth equation in (24), a polynomial equation of degree four is obtained in the unknown x_1. For each of the four solutions in x_1, finally x_2 and x_5 are easily computed while x_4 is obtained from the second equation and x_6 from the fifth equation in (24), respectively; in this way, four quintuples $\{x_1, x_2, x_4, x_5, x_6\}$ are computed. Obviously, other four quintuples $\{x_1, x_2, x_4, x_5, x_6\}$ are obtained starting from $x_{3,2}$.

4 Case study

The proposed approach has been applied to design a rotor position tracking controller for an induction motor whose parameter values are reported in Table I. To test the robustness of the control law, we have considered an induction motor driving a single-link robotic load which is modeled as a metal bar link. The parameter J which appears in (1) can be expressed as

$$J = J_m + \frac{1}{3}mL_0^2$$

where $m = 0.4\,\text{kg}$ is the link mass and $L_0 = 0.2\,\text{m}$ is the link length. Concerning the load disturbance T_l, it can be supposed dependent on the rotor position, according to the following law:

$$T_l = \frac{1}{2}mgL_0\sin\theta$$

in which g is the gravity acceleration. Note that this disturbance is not exogenous for our system; however, it is common practice in independent joint control of robotic systems to regard this type of dynamical load as if it were an exogenous disturbance (see, e.g., [11]).

Figure 1 shows the block scheme of the implemented system. The digital control architecture works at a sampling period T_c equal to $100\,\mu$s.

The design of the position tracking controller requires to find, for each of the two subsystems $\Sigma_{\rm el}$ and $\Sigma_{\rm mec}$, the matrix $\boldsymbol{X}$ solution of the Riccati's equation (11).

P	=	3	kW	L_r	=	0.149	H
V	=	220	V (rms)	M	=	0.143	H
$\omega_{\rm nom}$	=	305	rad/s	R_r	=	1.26	Ω
$\phi_{\rm nom}$	=	1.13	Wb	J_m	=	0.00448	Nms^2/rad
p	=	1	–	R_s	=	1.05	Ω
				L_s	=	0.149	H

Table I: Induction motor parameters.

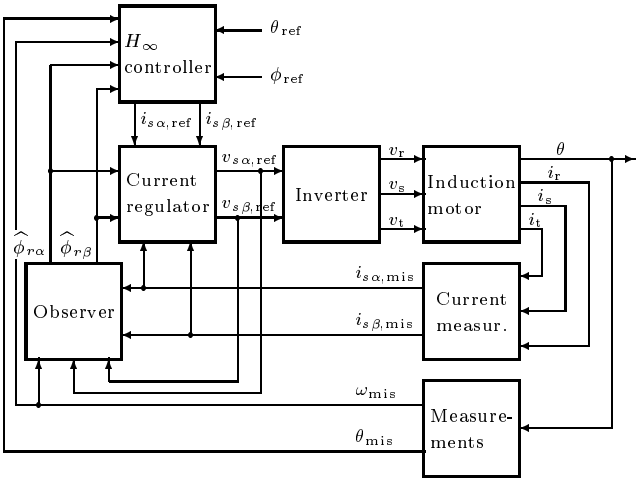

Figure 1: Block scheme of the simulated control scheme.

4.1 Controller design for the electrical and mechanical subsystems

Let first consider the subsystem $\Sigma_{\rm el}$ for which $d_{\rm el} = 0.1$ is assumed. In order to find a triple $\{x_1, x_2, x_3\}$ which solves system (18) and leads to a positive definite matrix $\boldsymbol{X}$, the expressions (19) are used to compute the functions $x_1(\lambda)$ and $|\boldsymbol{X}(\lambda)|$ in Λ which are plotted in Figure 2 for the case of negative sign chosen for both the x_2 and the x_1 solutions. It can be recognized that the positive definiteness constraint is satisfied with λ in the interval $\Lambda_{\rm ad} =]-1, 0[$ which is the whole interval of admissible values for λ. Since the upper bound on λ does not belong to $\Lambda_{\rm ad}$, the factor $\gamma_{\rm el}$ is lower-bounded by the value

$$\gamma^*_{\rm el} = \frac{\sqrt{2}d_{\rm el}L_r}{R_rM} = 0.117$$

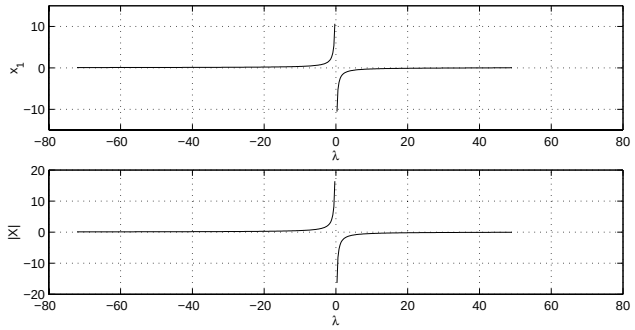

Figure 2: Plot of the functions $x_1(\lambda)$ and $|\boldsymbol{X}(\lambda)|$ for the subsystem $\Sigma_{\rm el}$: case of negative sign chosen for both the x_2 and the x_1 solutions to (18).

that cannot be achieved ($\lambda = 0$); therefore, a suboptimal solution can be adopted. To this aim let consider the closed-loop bandwidth whose expression is:

$$\mathrm{B_{el}} = \frac{\sqrt{\frac{MR_r}{L_r}K_{2,\mathrm{el}}}}{2\pi}\sqrt{-\beta_{\mathrm{el}} + \sqrt{\beta_{\mathrm{el}}^2 + 1}} \qquad (25)$$

where

$$\beta_{\mathrm{el}} = 2\,\zeta_{\mathrm{el}}^2 - 1 - \frac{1}{(\zeta_{\mathrm{el}}\,\mu_{\mathrm{el}})2},$$

and the coefficients ζ_{el} and μ_{el} are given by:

$$\begin{aligned} \zeta_{\mathrm{el}} &= \frac{1}{2}(1 + M\,K_{1,\mathrm{el}})\sqrt{\frac{R_r}{ML_rK_{2,\mathrm{el}}}}, \\ \mu_{\mathrm{el}} &= \frac{K_{2,\mathrm{el}}}{K_{1,\mathrm{el}}}\,\frac{L_r}{R_r}\,\frac{2}{(1 + M\,K_{1,\mathrm{el}})} \end{aligned} \qquad (26)$$

In (25) and (26) $K_{1,\mathrm{el}}$ and $K_{2,\mathrm{el}}$ are the elements of the gains matrix $\boldsymbol{K}_{\mathrm{el}}$. The expression (25) gives the closed-loop bandwidth's value of the subsystem as a function of $K_{1,\mathrm{el}}$ and $K_{2,\mathrm{el}}$. In this way, by means of a numerical approach, for each value of γ_{el} spanning the interval $]\gamma_{\mathrm{el}}^*,\ \gamma_{\mathrm{el,max}}]$, where $\gamma_{\mathrm{el,max}} = 1$ is assumed, one obtains a triple of values ($K_{1,\mathrm{el}}$, $K_{2,\mathrm{el}}$, $\mathrm{B_{el}}$). Collecting all the obtained triples it is then possible to build the plots of the functions $\gamma_{\mathrm{el}}(\mathrm{B_{el}})$, $K_{1,\mathrm{el}}(\mathrm{B_{el}})$ and $K_{2,\mathrm{el}}(\mathrm{B_{el}})$ which are represented in Figure 3. This result gives a effective tool to designing the H_∞ controller. In fact, for an assigned closed-loop bandwidth'value, both the corresponding attenuation factor γ_{el} and the controller gains are easily determined from Figure 3. In our case, imposing a desired bandwidth value equal to 4 Hz one obtains:

$$\gamma_{\mathrm{el}} = 0.123 \qquad \boldsymbol{K}_{\mathrm{el}} = (25.4 \quad 105).$$

Let now consider the mechanical subsystem Σ_{mec}, for which $d_{\mathrm{mec}} = 0.1$ is assumed. In this case, the parameter δ is restricted to the interval $\Delta =]-2, 1]$. A sextuple $\{x_1, x_2, x_3, x_4, x_5, x_6\}$ which solves system (24) and leads to a definite positive matrix $\boldsymbol{X}$, can be found if a plot of the functions $x_1(\delta)$, $|\boldsymbol{X}_2(\delta)|$ and $|\boldsymbol{X}(\delta)|$, with δ spanning the interval Δ is build, where $|\boldsymbol{X}_2|$ stands for the second-order principal minor of $\boldsymbol{X}$. In

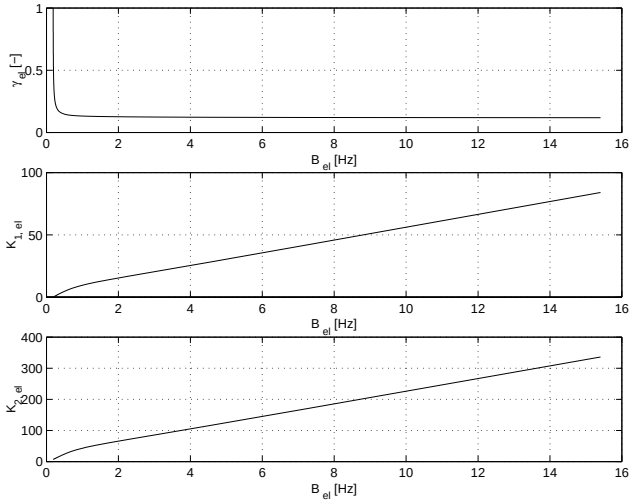

Figure 3: Plot of the functions $\gamma_{\mathrm{el}}(\mathrm{B_{el}})$, $K_{1,\mathrm{el}}(\mathrm{B_{el}})$ and $K_{2,\mathrm{el}}(\mathrm{B_{el}})$.

fact this plot allows visual inspection of the values of δ that satisfy the positive definiteness constraints; among these values of δ, the maximum one is chosen. Figure (4) shows the plot of the functions $x_1(\delta)$, $|\boldsymbol{X}_2(\delta)|$ and $|\boldsymbol{X}(\delta)|$ when the second solution is chosen both for x_3 and x_1. It can be recognized that the positive definiteness constraint is satisfied if $\delta \in \Delta_{\mathrm{ad}} =]-2, 0[$. Since the upper bound on δ does not belong to Δ_{ad}, the factor δ_{mec} is lower-bounded by the value

$$\delta_{\mathrm{mec}}^* = \frac{d_{\mathrm{mec}}\sqrt{3(1 + J^2)}}{k_T} = 0.180$$

that cannot be achieved ($\delta = 0$); therefore, a suboptimal solution can be found according the same procedure outlined for the electrical subsystem. In detail, for each value of δ spanning the interval Δ_{ad}, the values of $K_{1,\mathrm{mec}}$, $K_{2,\mathrm{mec}}$, $K_{3,\mathrm{mec}}$ are calculated from equation (13). Plugging these values in the following expression

$$\frac{\Theta_{\mathrm{ref}}(s)}{\Theta(s)} = \frac{\frac{k_T}{J}(K_{1,\mathrm{mec}}\,s^2 + K_{2,\mathrm{mec}}\,s + K_{3,\mathrm{mec}})}{s^3 + \frac{k_T}{J}(K_{1,\mathrm{mec}}\,s^2 + K_{2,\mathrm{mec}}\,s + K_{3,\mathrm{mec}})} \qquad (27)$$

which gives the transfer function of the closed-loop system, the corresponding value of $\mathrm{B_{mec}}$ is numerically computed. Collecting all the so-obtained quadruples, it is then possible to build the plots of the functions $\gamma_{\mathrm{mec}}(\mathrm{B_{mec}})$, and $\boldsymbol{K}_{\mathrm{mec}}(\mathrm{B_{mec}})$ which are represented in Figures 5 and 6, respectively. Since T_c is equal to 10 kHz we have set the closed-loop bandwidth to 600 Hz. This choice is mainly determined by requirement to reduce the effects produced by noise measurement. According with this choice one has:

$$\gamma_{\mathrm{mec}} = 0.204 \qquad \boldsymbol{K}_{\mathrm{mec}} = (37.7 \quad 3409.8 \quad 30.4).$$

The desired rotor position trajectory was selected as:

$$\theta_{\mathrm{ref}}(t) = 10\pi e^{-0.2\,t}\sin^2(\pi\,t) \quad \mathrm{rad};$$

while the reference trajectory of the flux norm is kept constant at its nominal value. To avoid the start-up

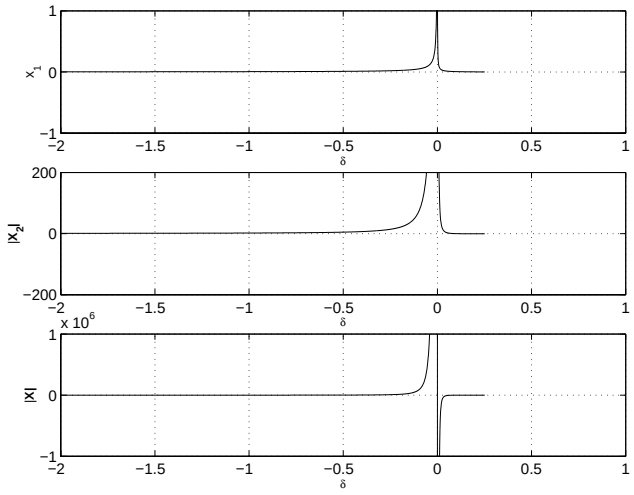

Figure 4: Plot of the functions $x_1(\delta)$, $|\boldsymbol{X}_2(\delta)|$ and $|\boldsymbol{X}(\delta)|$ for the subsystem $\Sigma_{\rm mec}$ when the second solution is chosen both for x_3 and x_1.

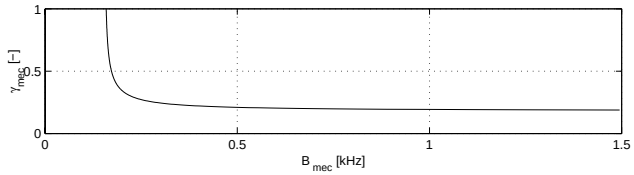

Figure 5: Plot of the function $\gamma_{\rm mec}(\mathrm{B}_{\rm mec})$.

singularity in (2), the initial conditions of the flux estimates are set to

$$\widehat{\phi}_{r\alpha}(0) = 0.001 \qquad \widehat{\phi}_{r\beta}(0) = 0.0$$

The resulting position tracking error is shown in Figure 7. The very good performance of the control system in terms of both position tracking and, at same time, load torque disturbance rejection capability is evident.

5 Conclusion

A systematic procedure to designing a rotor position tracking H_∞ controller has been developed. This represents a powerful design tool since it enables to choose the controller gains starting from requirements imposed on the control system bandwidth. The design has been illustrated for a joint servo of a single robotic link.

References

[1] P. Aquino, M. Feemster, D. M. Dawson, and A. Behal "Adaptive partial state feedback control of the induction motor: elimination of rotor flux and rotor velocity measurements," *IEEE Conf. Decision & Control*, Tampa, FL, pp. 977–982, 1998.

[2] C. Canudas de Wit, R. Ortega and S.I. Seleme, "Robot motion control using induction motor drive," *IEEE Trans. Robotics & Automation* , vol. 2, pp. 533–538, 1993.

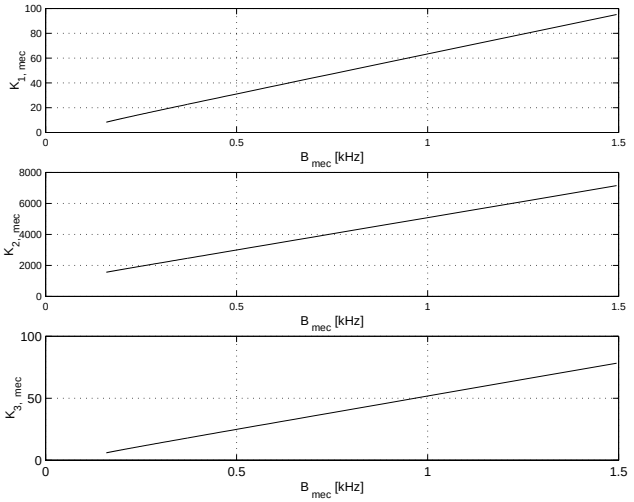

Figure 6: Plot of the functions $K_{1,\rm mec}(\mathrm{B}_{\rm mec})$, $K_{2,\rm mec}(\mathrm{B}_{\rm mec})$, and $K_{3,\rm mec}(\mathrm{B}_{\rm mec})$.

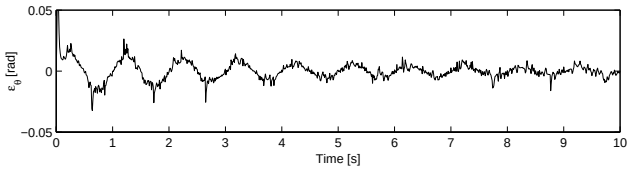

Figure 7: Rotor position tracking error.

[3] C. Canudas de Wit and S.I. Seleme, "Robust torque regulation for induction motors: the minimum energy approach," *Automatica*, vol. 33, n. 1, pp. 63–79, 1997.

[4] S. Chiaverini, G. Figalli, and G. Fusco, "H_∞ design of a robust speed controller for induction motors," *IEEE Conf. Control Applications*, pp. 956–961, Hawaii, HI, Aug. 1999.

[5] D. M. Dawson, J. Hu, and P. Vedagarbha, "An adaptive controller for a class of induction motor systems," *IEEE Conf. Decision & Control*, New Orleans, LA, pp. 1567–1572, 1995.

[6] J.C. Doyle, K. Glover, P.P. Khargonekar, and B.A. Francis, "State space solutions to standard H_2 and H_∞ control problems," *IEEE Trans. Automatic Control*, vol. 34, pp. 831–846, 1989.

[7] M. Feemster, D. M. Dawson, P. Aquino,and D. Haste "Position tracking of the induction motor without rotor velocity or rotor flux measurements," *IEEE Int. Conf. Control Applications*, Trieste, I, pp. 36–40, 1998.

[8] G. Fusco, "An H_∞ position tracking controller for induction motors" *IEEE American Control Conf.*, Chicago, IL, USA, June 2000.

[9] D. Georges and C. Canudas de Wit, "Nonlinear H_2 and H_∞ optimal controllers for current fed induction motors," *European Control Conf.*, Bruxelles, B, vol. 1, 1997.

[10] J. Hu, D. M. Dawson, and Y. Qian, "Position tracking control for robot manipulators driven by induction without flux measurements," *IEEE Trans. Robotics & Automation*, vol. 12, pp. 419–438, 1996.

[11] L. Sciavicco and B. Siciliano, *Modeling and Control of Robot Manipulators*, Springer-Verlag, London, UK, 2000.

[12] W.J. Wang and C.C. Wang, "A new composite adaptive speed controller for induction motor based on the feedback linearization," *IEEE Trans. Energy Conversion*, vol. 13, pp. 1–6, 1998.